

Predictions on the neutrinoless double beta decay from the leptogenesis via the LH_u flat direction

Masaaki Fujii¹, K. Hamaguchi¹, and T. Yanagida^{1,2}

¹ *Department of Physics, University of Tokyo, Tokyo 113-0033, Japan*

² *Research Center for the Early Universe, University of Tokyo, Tokyo, 113-0033, Japan*

Abstract

If the baryon asymmetry in the present universe is generated by decays of the LH_u flat direction, the observed baryon asymmetry requires the mass of the lightest neutrino to be much smaller than the mass scale indicated from the atmospheric and solar neutrino oscillations. Such a small mass of the lightest neutrino leads to a high predictability on the rate of the neutrinoless double beta ($0\nu\beta\beta$) decay. In this letter we show general predictions on the $0\nu\beta\beta$ decay in the leptogenesis via the LH_u flat direction.

¹UT-999

1 Introduction

Leptogenesis [1] has been widely considered as an attractive mechanism to account for the baryon asymmetry in the present universe, especially after the Super-Kamiokande Collaboration reported the evidence of the atmospheric neutrino oscillation [2]. In particular, the leptogenesis via the LH_u flat direction [3], based on the Affleck-Dine mechanism [4], seems to work naturally in the supersymmetric (SUSY) standard model. Recently, we have performed detailed analyses on this leptogenesis mechanism via the LH_u flat direction, taking into account the relevant thermal effects [5, 6],¹ and have shown that the generated baryon asymmetry is determined almost only by the mass of the lightest neutrino m_ν [6]. In order to explain the empirical baryon asymmetry in the present universe, the mass of the lightest neutrino should be much smaller than the mass scale of the atmospheric and solar neutrino oscillations. This fact leads to a high predictability on the rate of the neutrinoless double beta ($0\nu\beta\beta$) decay [6].

In the previous work, we have assumed the normal hierarchy in the neutrino mass spectrum. In this letter, we investigate predictions on the $0\nu\beta\beta$ decay in the more general cases including the inverted hierarchy in neutrino masses. As we will see, it is quite interesting that the predicted value of the mass parameter $m_{\nu_e\nu_e}$ is in the accessible range of future experiments [9, 10, 11, 12, 13, 14, 15] of the $0\nu\beta\beta$ decay.

2 Leptogenesis via the LH_u flat direction

In this section we briefly review the leptogenesis via the LH_u flat direction [3, 5, 6, 16]. Let us start by writing down the effective dimension-five operator in the superpotential,

$$W = \frac{1}{2M_i} (L_i H_u) (L_i H_u) , \quad (1)$$

which induces small neutrino masses m_{ν_i} [17] after the neutral component of the Higgs field H_u obtains its vacuum expectation value $\langle H_u \rangle = 174 \text{ GeV} \times \sin \beta$,²

$$m_{\nu_i} = \frac{\langle H_u \rangle^2}{M_i} , \quad (2)$$

¹The thermal effects can be avoided if we assume a gauged $U(1)_{B-L}$ [7] or a low scale inflation [8].

² $\tan \beta$ is defined as $\tan \beta \equiv \langle H_u \rangle / \langle H_d \rangle$, where H_u and H_d are the Higgs fields which provide masses for the up- and down-type quarks, respectively.

where we have taken a basis in which the neutrino mass matrix is diagonal. We adopt the following supersymmetric D-flat direction [3]:

$$\tilde{L} = \frac{1}{\sqrt{2}} \begin{pmatrix} \phi \\ 0 \end{pmatrix}, \quad H_u = \frac{1}{\sqrt{2}} \begin{pmatrix} 0 \\ \phi \end{pmatrix}. \quad (3)$$

Here and hereafter, we suppress the family index i . As we will see below, the flat direction which generates the lepton asymmetry most effectively corresponds to the *lightest* neutrino.

The total scalar potential for the flat direction field ϕ is given by

$$\begin{aligned} V(\phi) = & m_\phi^2 |\phi|^2 + \frac{m_{3/2}}{8M} (a_m \phi^4 + H.c.) \\ & - c_H H^2 |\phi|^2 + \frac{H}{8M} (a_H \phi^4 + H.c.) \\ & + \sum_{f_k |\phi| < T} c_k f_k^2 T^2 |\phi|^2 + a_g \alpha_S(T)^2 T^4 \ln \left(\frac{|\phi|^2}{T^2} \right) \\ & + \frac{1}{4M^2} |\phi|^6. \end{aligned} \quad (4)$$

Here, the potential terms in the first line comes from the SUSY breaking at the zero temperature $T = 0$, which are mediated by supergravity, and we take $m_\phi \simeq m_{3/2} |a_m| \simeq 1$ TeV, hereafter.³ The terms in the second line, depending on the Hubble parameter H , reflects the additional SUSY breaking effects caused by the finite energy density of the inflaton [18]. Hereafter, we take $c_H \simeq 1 (> 0)$ and $|a_H| \simeq 1$. The terms in the third line represent the effects of the finite temperature [19, 5, 20, 6]. Here, f_k represent Yukawa and gauge coupling constants of the field ϕ , α_S is the gauge coupling constant of the $SU(3)_C$, and c_k and a_g are coefficients of order unity.⁴ Finally, the last term directly comes from the superpotential in Eq. (1).

During the inflation, the negative Hubble mass term $-c_H H^2 |\phi|^2$ causes an instability of the flat direction field ϕ around the origin ($\phi \simeq 0$), and ϕ field runs to one of the following four minima of the potential:

$$|\phi| \simeq \sqrt{MH}, \quad (5)$$

$$\arg(\phi) \simeq \frac{-\arg(a_H) + (2n+1)\pi}{4}, \quad n = 0 \cdots 3, \quad (6)$$

which are the balance points between the Hubble-induced terms and the $|\phi|^6$ term.

After the inflation, the amplitude of the ϕ field starts to be reduced following the gradual decrease of the Hubble parameter H [see Eq. (5)], and eventually, either thermal

³We assume gravity mediated SUSY breaking models.

⁴The list of c_k and f_k is given in Ref. [5]. In the case of LH_u flat direction, a_g is given by $a_g = 9/8$.

terms $T^2|\phi|^2$ or $T^4\ln(|\phi|^2)$, or the soft mass term $m_\phi^2|\phi|^2$ dominate the scalar potential, which causes a coherent oscillation of the ϕ around the origin. At this stage, the difference between the phases of the complex couplings a_m and a_H leads to a phase rotational motion of ϕ , which results in generation of the lepton asymmetry, $n_L = (1/2)i(\dot{\phi}^*\phi - \phi^*\dot{\phi})$. Decay of ϕ produces the lepton asymmetry in the thermal bath and a part of the produced lepton asymmetry is then converted into the baryon asymmetry [1] via the sphaleron effects [21].

We show the result of detailed calculation [6] in Fig. 2, which presents the contour plot of the baryon asymmetry in the neutrino mass (m_ν) – reheating temperature (T_R) plane. As can be seen in Fig. 2, the baryon asymmetry is almost independent of the reheating temperature T_R , and is determined only by the mass of the lightest neutrino m_ν for $T_R \gtrsim 10^5$ GeV. Thus, the baryon asymmetry in the present universe $n_B/s \simeq (0.4-1) \times 10^{-10}$ indicates the mass of the lightest neutrino to be

$$m_\nu \simeq (0.1 - 3) \times 10^{-9} \text{ eV} \quad (7)$$

in a wide range of the reheating temperature $10^5 \text{ GeV} \lesssim T_R \lesssim 10^{12} \text{ GeV}$.⁵

3 Prediction on the $0\nu\beta\beta$ decay

The neutrinoless double beta ($0\nu\beta\beta$) decay, if observed, is the strongest evidence for lepton number violation. In other words, it suggests the Majorana character of the neutrinos and thus the existence of the nonrenormalizable operator given in Eq.(1), which is a crucial ingredient for our leptogenesis to work.

In the present scenario, as explained in the previous section, the observed baryon asymmetry in the universe is mainly determined by the mass of the lightest neutrino, $m_\nu \sim 10^{-9} \text{ eV}$, regardless of the reheating temperature of inflation. This small neutrino mass predicted from the leptogenesis, combined with the atmospheric and solar neutrino oscillation experiments, allows us to have definite predictions on the rate of the $0\nu\beta\beta$ decay. This is a clear contrast to the other baryo/leptogenesis scenarios which heavily rely on various unknown parameters in high energy physics.

In our previous publication [6], we have assumed the normal mass hierarchy for the light neutrinos. In this letter, we investigate general predictions on the $0\nu\beta\beta$ decay taking into account of the case of inverted mass hierarchy for neutrinos.

⁵If the $U(1)_{B-L}$ symmetry is gauged in high energy scale, the resultant baryon asymmetry is enhanced in the “D-term stopping case” [7]. However, even in this case, the required mass of the lightest neutrino must satisfy $m_\nu \lesssim 10^{-5} \text{ eV}$ to avoid the cosmological gravitino problem, and the prediction on the $0\nu\beta\beta$ decay is almost the same as that presented in this letter.

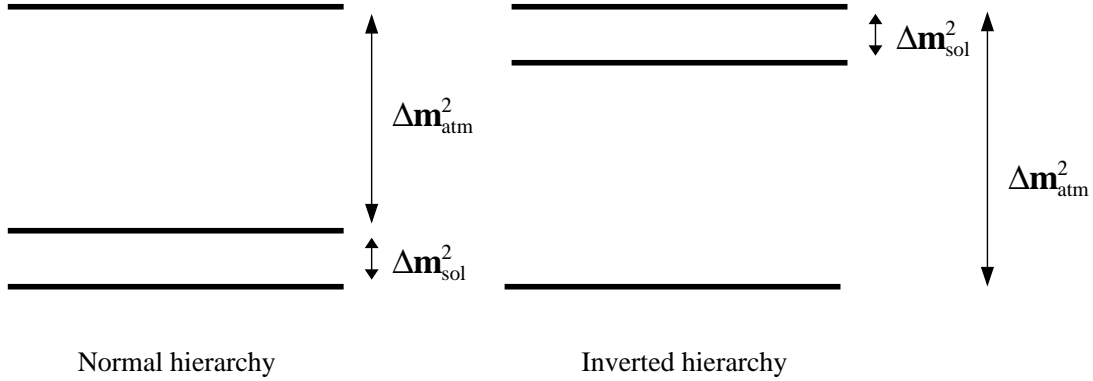


Figure 1: Hierarchies in the neutrino mass spectrum.

The most important ingredient to determine the rate of the $0\nu\beta\beta$ decay is the effective mass of the electron-type neutrino, which is given by

$$|m_{\nu_e\nu_e}| = |U_{e1}^2 m_{\nu_1} + U_{e2}^2 m_{\nu_2} + U_{e3}^2 m_{\nu_3}|, \quad (8)$$

where m_{ν_i} 's are the mass eigenvalues of the neutrinos. $U_{\alpha i}$ is the mixing matrix which diagonalizes the neutrino mass matrix, where $\alpha = e, \mu, \tau$ represent the weak eigenstates. Here, we take a basis in which the mass matrix of the charged lepton is diagonal.

In general, the mass pattern for the neutrinos can be classified into the two cases; the normal mass hierarchy and the inverted mass hierarchy, which are presented in Fig. 1. In this letter, we label the each mass eigenstates in the following way; $m_{\nu_1} < m_{\nu_2} < m_{\nu_3}$ for the case of the normal mass hierarchy, and $m_{\nu_3} < m_{\nu_1} < m_{\nu_2}$ for the case of the inverted mass hierarchy. Then, the observed mass squared differences are given by

$$\Delta m_{\text{atm}}^2 = |m_{\nu_3}^2 - m_{\nu_2}^2|, \quad \Delta m_{\text{sol}}^2 = m_{\nu_2}^2 - m_{\nu_1}^2, \quad (9)$$

for the atmospheric and the solar neutrino oscillations, respectively. By taking this convention, we can treat the mixing angles of the neutrinos in a similar way for both cases of the neutrino mass hierarchies. The mixing matrix $U_{\alpha i}$ is parameterized as

$$U_{\alpha i} = \begin{pmatrix} c_{12}c_{13} & s_{12}c_{13} & s_{13}e^{-i\delta} \\ -s_{12}c_{23} - c_{12}s_{23}s_{13}e^{i\delta} & c_{12}c_{23} - s_{12}s_{23}s_{13}e^{i\delta} & s_{23}c_{13} \\ s_{12}s_{23} - c_{12}c_{23}s_{13}e^{i\delta} & -c_{12}s_{23} - s_{12}c_{23}s_{13}e^{i\delta} & c_{23}c_{13} \end{pmatrix} \cdot P, \quad (10)$$

where $c_{ij} \equiv \cos\theta_{ij}$, $s_{ij} \equiv \sin\theta_{ij}$ and $P = \text{diag}(1, e^{i\beta}, e^{i\gamma})$. δ is a Dirac-type phase and β, γ are two phases associated with the Majorana character of the neutrinos. By virtue of our convention, the θ_{23} and θ_{12} always correspond to the mixing angles for the atmospheric and the solar neutrino oscillations, respectively, regardless of the type of mass hierarchy for the neutrinos. In addition, the element of the mixing matrix U constrained by the CHOOZ experiment is always correspond to $(e, 3)$ element as $|U_{e3}| \lesssim 0.15$ [22].

The requirement for our leptogenesis to explain the observed baryon asymmetry is that the mass of the lightest neutrino is to be $m_\nu \sim 10^{-9}$ eV, which is negligibly small compared with the other two mass eigenvalues of the neutrinos. This immediately leads to the following upper and lower bounds on the electron-type neutrino mass:

$$| |U_{e2}|^2 m_{\nu_2} - |U_{e3}|^2 m_{\nu_3} | \leq |m_{\nu_e \nu_e}| \leq |U_{e2}|^2 m_{\nu_2} + |U_{e3}|^2 m_{\nu_3} , \quad (11)$$

$$| |U_{e1}|^2 m_{\nu_1} - |U_{e2}|^2 m_{\nu_2} | \leq |m_{\nu_e \nu_e}| \leq |U_{e1}|^2 m_{\nu_1} + |U_{e2}|^2 m_{\nu_2} \quad (12)$$

for the normal and the inverted mass hierarchies, respectively.

The predictions on the $0\nu\beta\beta$ decay in the case of the normal mass hierarchy have been investigated in detail in Ref. [6]. The upper and lower bounds on the electron-type neutrino mass in Eq. (11) can be written as

$$|m_{\nu_e \nu_e}|_{\min}^{\max} \simeq s_{12}^2 \sqrt{\Delta m_{\text{sol}}^2} \pm |U_{e3}|^2 \sqrt{\Delta m_{\text{atm}}^2} . \quad (13)$$

In Fig. 3, we present the numerical result for the case of the large mixing angle (LMA) solution. The red (solid) and blue (dashed) lines correspond to the cases where $|U_{e3}| = 0.15$ and $|U_{e3}| = 0.05$, respectively. As for the mass squared differences, we have adopted the following best fit values [2, 23]:

$$\Delta m_{\text{atm}}^2 = 3.2 \times 10^{-3} \text{ eV}^2 , \quad \Delta m_{\text{sol}}^2 = 4.9 \times 10^{-5} \text{ eV}^2 . \quad (14)$$

The green (vertical) line denotes the best fit values of the mixing angle $\tan^2 \theta_{12} = 0.37$. The behavior of the bounds when we vary the mass squared differences Δm_{atm}^2 and Δm_{sol}^2 is easily seen from the Eq. (13). We see that the overall scale of the $|m_{\nu_e \nu_e}|$ is almost proportional to the $\sqrt{\Delta m_{\text{sol}}^2}$. For example, when we vary the Δm_{sol}^2 within the 95% C.L. allowed region of the LMA solution, $|m_{\nu_e \nu_e}|$ changes within about $\times / \div 1.7$ of the value presented in Fig. 3. As clearly shown in this figure, the $|m_{\nu_e \nu_e}|$ is predicted in a narrow range when the $|U_{e3}|$ is much smaller than the present bound.

Now, let us consider the case of the inverted mass hierarchy for the neutrinos. The Eq. (12) can be written in terms of the observables in neutrino oscillation experiments as

$$|m_{\nu_e \nu_e}|_{\max} \simeq (1 - |U_{e3}|^2) \sqrt{\Delta m_{\text{atm}}^2} \left(1 - \frac{\Delta m_{\text{sol}}^2}{2\Delta m_{\text{atm}}^2} c_{12}^2 \right) , \quad (15)$$

$$|m_{\nu_e \nu_e}|_{\min} \simeq (1 - |U_{e3}|^2) \sqrt{\Delta m_{\text{atm}}^2} c_{12}^2 \left| \left((1 - \tan^2 \theta_{12}) - \frac{\Delta m_{\text{sol}}^2}{2\Delta m_{\text{atm}}^2} \right) \right| , \quad (16)$$

for the upper and lower bounds, respectively. As seen from these relations, the mass squared differences for the solar neutrino oscillations Δm_{sol}^2 gives negligible effects on

the upper bound of $|m_{\nu_e\nu_e}|$. The Δm_{sol}^2 affects the lower bound of the $|m_{\nu_e\nu_e}|$ only when the following relation is satisfied:

$$|(1 - \tan^2\theta_{12})| \lesssim \frac{\Delta m_{\text{sol}}^2}{\Delta m_{\text{atm}}^2}. \quad (17)$$

In Fig. 4, we present the upper and the lower bounds on the $|m_{\nu_e\nu_e}|$ in the case of the inverted mass hierarchy. Here, we have used the $|U_{e3}| = 0.15$. As for the mass squared differences, we have adopted the best fit values for the LMA solution as before. However, this result is applicable to the other solutions for the solar neutrino oscillations except for the case of $\tan^2\theta_{12} \simeq 1$, because of the reason mentioned above. The two green (vertical) lines correspond to the best fit values of the mixing angles for the LMA and the LOW solutions ($\tan^2\theta_{12} = 0.37, 0.68$) [23] from left to right, respectively. As seen from the figure, the $|m_{\nu_e\nu_e}|$ is restricted in a very small range such as $0.01 \text{ eV} \lesssim |m_{\nu_e\nu_e}| \lesssim 0.06 \text{ eV}$ when $\tan^2\theta_{12} \lesssim 0.7$, which is clearly in the reach of the future $0\nu\beta\beta$ decay experiments. Even if we change the Δm_{atm}^2 within the 99% C.L. allowed region, the overall scale of the $|m_{\nu_e\nu_e}|$ varies within only $\times/\div 1.5$ of the value presented in Fig. 4.

4 Conclusions

Leptogenesis via the LH_u flat direction is one of the most interesting scenarios to explain the observed baryon asymmetry, in which the observed baryon asymmetry has a direct connection to the mass of the lightest neutrino regardless of the details of high energy physics. In this letter, we have derived predictions on the rate of the $0\nu\beta\beta$ decay, which is regarded as a low energy consequence of the present leptogenesis; the mass of the lightest neutrino must be $m_\nu \sim 10^{-9} \text{ eV}$.

Both in the cases of the normal and the inverted mass hierarchies for the neutrinos, the region of $|m_{\nu_e\nu_e}|$ is strongly restricted and it is accessible in the future $0\nu\beta\beta$ decay experiments [9, 10, 11, 12, 13, 14, 15]. Furthermore, predictions on the $|m_{\nu_e\nu_e}|$ become much more definite when the $|U_{e3}|$ is severely constrained (for the case of the normal hierarchy) or the mixing angle for the solar neutrino oscillation is restricted as $\tan^2\theta_{12} < 1$ (for the case of the inverted hierarchy) in the future experiments. The predictions on the $0\nu\beta\beta$ decay derived in this letter will play a crucial role on testing the leptogenesis via the LH_u flat direction.

References

- [1] M. Fukugita and T. Yanagida, Phys. Lett. B**174** (1986) 45.

- [2] Y. Fukuda *et al.* [Super-Kamiokande Collaboration],
 Phys. Lett. B**433** (1998) 9 [arXiv:hep-ex/9803006];
 Phys. Lett. B**436** (1998) 33 [arXiv:hep-ex/9805006];
 Phys. Rev. Lett. **81** (1998) 1562 [arXiv:hep-ex/9807003].
 See also a recent data,
 C. Yanagisawa, Nucl. Phys. Proc. Suppl. **95** (2001) 93.
- [3] H. Murayama and T. Yanagida, Phys. Lett. B**322** (1994) 349 [arXiv:hep-ph/9310297].
- [4] I. Affleck and M. Dine, Nucl. Phys. B**249** (1985) 361.
- [5] T. Asaka, M. Fujii, K. Hamaguchi and T. Yanagida, Phys. Rev. D**62** (2000) 123514 [arXiv:hep-ph/0008041].
- [6] M. Fujii, K. Hamaguchi and T. Yanagida, Phys. Rev. D**63** (2001) 123513 [arXiv:hep-ph/0102187].
- [7] M. Fujii, K. Hamaguchi and T. Yanagida, Phys. Rev. D**65** (2002) 043511 [arXiv:hep-ph/0109154].
- [8] T. Asaka, Phys. Lett. B**521** (2001) 329 [arXiv:hep-ph/0110073].
- [9] H. V. Klapdor-Kleingrothaus *et al.* [GENIUS Collaboration], arXiv:hep-ph/9910205;
 H. V. Klapdor-Kleingrothaus, arXiv:hep-ph/0104028.
- [10] E. Fiorini, Phys. Rept. **307** (1998) 309; Nucl. Phys. Proc. Suppl. **100** (2001) 332;
 A. Alessandrello *et al.* [CUORE Collaboration], arXiv:hep-ex/0201038.
- [11] H. Ejiri, J. Engel, R. Hazama, P. Krastev, N. Kudomi and R. G. Robertson, Phys. Rev. Lett. **85** (2000) 2917 [arXiv:nucl-ex/9911008].
- [12] S. Moriyama, Talk at International Workshop on Technology and Application of Xenon Detectors (Xenon01), ICRR, Kashiwa, Japan, December 3-4, 2001.
- [13] S. Waldman, Talk at International Workshop on Technology and Application of Xenon Detectors (Xenon01), ICRR, Kashiwa, Japan, December 3-4, 2001.
- [14] C. E. Aalseth *et al.* [Majorana Collaboration], arXiv:hep-ex/0201021.
- [15] For a recent review and references, see S. R. Elliott and P. Vogel, arXiv:hep-ph/0202264.
- [16] T. Moroi and H. Murayama, JHEP **0007** (2000) 009 [arXiv:hep-ph/9908223].
- [17] T. Yanagida, in Proceedings of the “*Workshop on the Unified Theory and the Baryon Number in the Universe*”, Tsukuba, Japan, 1979, edited by O. Sawada and A. Sugamoto (KEK Report No. KEK-79-18), p. 95; Prog. Theor. Phys. **64** (1980) 1103;
 M. Gell-Mann, P. Ramond and R. Slansky, in “*Supergravity*”, edited by D.Z. Freedman and P. van Nieuwenhuizen (North-Holland, Amsterdam, 1979).

- [18] M. Dine, L. Randall and S. Thomas, Phys. Rev. Lett. **75** (1995) 398 [arXiv:hep-ph/9503303]. Nucl. Phys. B**458** (1996) 291 [arXiv:hep-ph/9507453].
- [19] R. Allahverdi, B. A. Campbell and J. Ellis, Nucl. Phys. B**579** (2000) 355 [arXiv:hep-ph/0001122].
- [20] A. Anisimov and M. Dine, arXiv:hep-ph/0008058;
See also, A. Anisimov, arXiv:hep-ph/0111233.
- [21] V. A. Kuzmin, V. A. Rubakov and M. E. Shaposhnikov, Phys. Lett. B**155** (1985) 36.
- [22] M. Apollonio *et al.*, Phys. Lett. B**466** (1999) 415 [arXiv:hep-ex/9907037].
- [23] G. L. Fogli, E. Lisi, D. Montanino and A. Palazzo, Phys. Rev. D**64** (2001) 093007 [arXiv:hep-ph/0106247];
G. L. Fogli, E. Lisi, A. Marrone, D. Montanino and A. Palazzo, arXiv:hep-ph/0201290, and references therein.

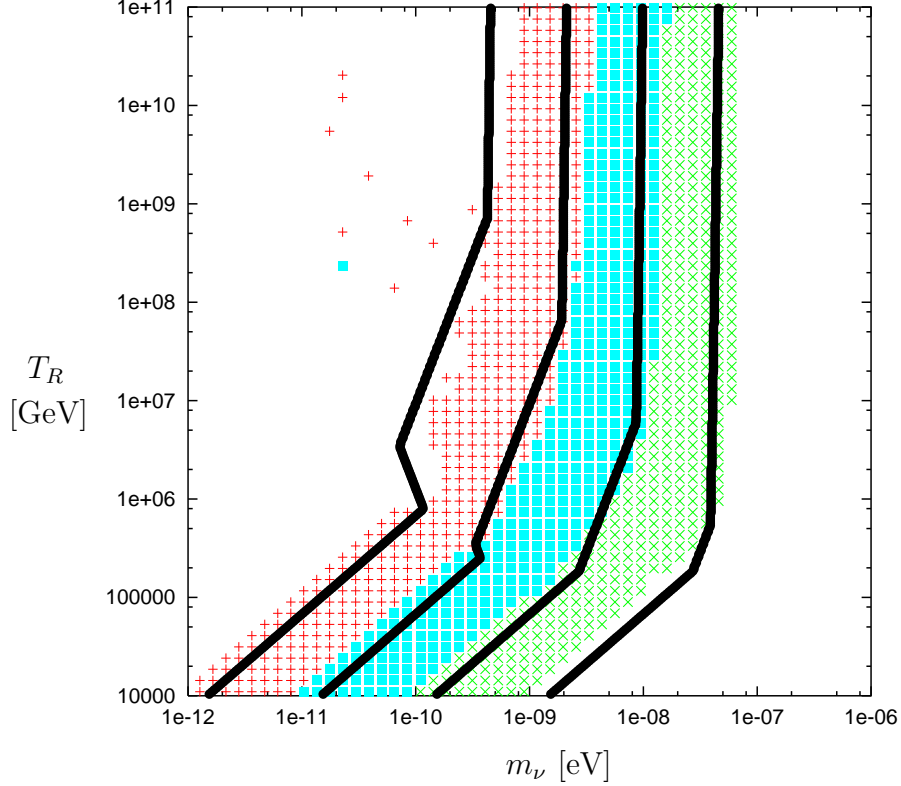


Figure 2: The plots of baryon asymmetries n_B/s in the m_ν - T_R plane. The solid lines are the contour plot of the n_B/s obtained by analytical calculation, which represent $n_B/s = 10^{-9}, 10^{-10}, 10^{-11}$, and 10^{-12} from the left to the right. The regions with points show the result of the numerical simulation, which represent $10^{-9} > n_B/s > 10^{-10}$, $10^{-10} > n_B/s > 10^{-11}$ and $10^{-11} > n_B/s > 10^{-12}$ from the left to the right. In the numerical simulation, we have taken $m_\phi = m_{3/2}|a_m| = 1$ TeV, $c_H = |a_H| = 1$, $\arg(a_m) = 0$ and $\arg(a_H) = \pi/3$.

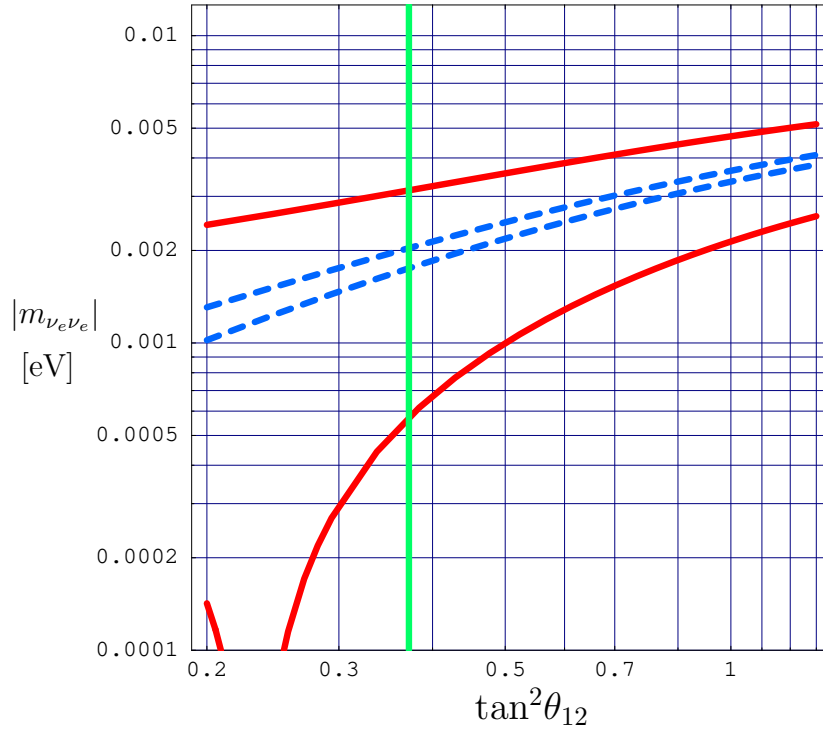


Figure 3: The upper and lower bands on the effective mass of the electron-type neutrino $|m_{\nu_e \nu_e}|$ in the case of the normal mass hierarchy. The red (solid) and blue (dashed) lines correspond to the cases where $|U_{e3}| = 0.15$ and $|U_{e3}| = 0.05$, respectively. As for the mass squared differences, we have adopted the best fit values. The green (vertical) line corresponds to the best fit values of $\tan^2 \theta_{12}$ for the LMA solution.

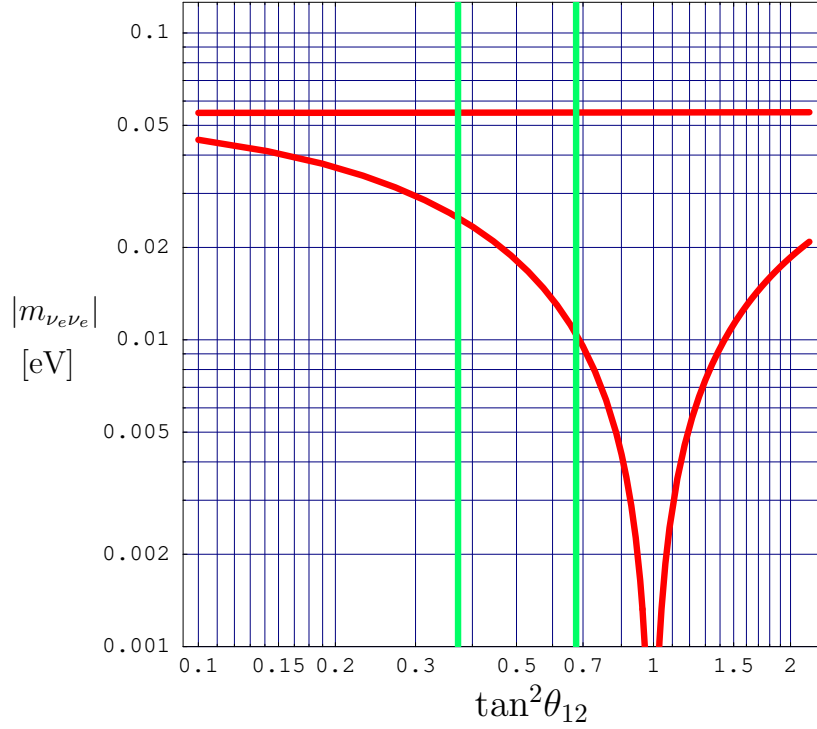


Figure 4: The upper and lower bands on the effective mass of the electron-type neutrino $|m_{\nu_e \nu_e}|$ in the case of the inverted mass hierarchy. Here, we have used the $|U_{e3}| = 0.15$. As for the mass squared differences, we have adopted the best fit values for the LMA solution given in Eq. (14). However, this result is applicable to the other solutions for the solar neutrino oscillations except for $\tan^2 \theta_{12} \simeq 1$ as explained in the text. The two green (vertical) lines correspond to the best fit values of the mixing angles for the LMA and the LOW solutions from left to right, respectively.